JOURNAL OF CATALYSIS **176,** 365–375 (1998)
ARTICLE NO. CA982066

Raman Spectroscopic and TPR Studies of Oxygen Species over BaO- and BaX_2(X = F, Cl, Br)-Promoted Nd_2O_3 Catalysts for the Oxidative Coupling of Methane

Peter C. T. Au,[1] Y. W. Liu, and C. F. Ng

Department of Chemistry and Centre for Surface Analysis and Research, Hong Kong Baptist University, Kowloon Tong, Hong Kong, China

Received October 31, 1997; revised March 5, 1998; accepted March 9, 1998

The 30 mol% BaO- and 30 mol% BaX_2(X = F, Cl, Br)-promoted Nd_2O_3 catalysts have been investigated for the oxidative coupling of methane (OCM). The addition of BaO or BaX_2 to Nd_2O_3 could obviously enhance the catalytic performance. We observed leaching of halide during the OCM reaction. The stability of the halide ions follows the order: $F^- > Cl^- > Br^-$. XRD and Raman results revealed that the addition of BaO or BaX_2 has significantly altered the surface and bulk natures of Nd_2O_3. The enlargement of Nd_2O_3 lattice in the BaO- and BaX_2-promoted Nd_2O_3 catalysts was due to ionic exchange between Ba^{2+} and Nd^{3+} or X^- and O^{2-} ions. Raman results showed that there were dioxygen species such as O_2^{2-}, O_2^{n-}, O_2^-, and $O_2^{\delta-}$ on the surface when BaO or BaX_2 was added to Nd_2O_3. We suggest that the lattice defects generated due to ionic exchanges could promote the formation of dioxygen adspecies. TPR results implied that, besides the dioxygen species, there were mono-oxygen species existing in these catalysts. By pulsing CH_4 over the catalysts, we found that both dioxygen and mono-oxygen species could activate CH_4 at high temperatures and the existence of dioxygen species could improve the catalytic performance, especially in the enhancement of C_2 selectivity and C_2H_4/C_2H_6 ratio.

INTRODUCTION

Oxygen species have been studied extensively in catalytic processes. Depending on the properties of the catalysts, the distribution of oxygen species varies. Osada *et al.* have studied the Y_2O_3–CaO catalyst for the OCM reaction (1). They found that the C_{2+} selectivity at 700°C was obviously enhanced with increasing Y_2O_3 contents; they attributed this to the formation of a solid solution accompanying the production of interstitial superoxide ions, O_2^-. Kaminsky *et al.* (2) and Au *et al.* (3, 4) reported that the addition of Ba^{2+} into Y_2O_3 could create charge-deficient oxygen sites in the Ba/Y_2O_3 catalysts. Au and Zhou have reported that active centres such as trapped electrons and anionic vacancies could be generated due to ionic exchanges in SrF_2/SmOF catalysts (5, 6) and the adsorption of O_2 on these centres would result in the production of O^-, O_2^{2-}, and O_2^- species. It has been proposed that besides the exchange between the cations, there was exchange between the F^- and O^{2-} ions and F^- was playing a role in the modification of the SmOF catalyst. The effects of other halide ions on the catalytic performance of the OCM reaction have been studied by many researchers (3, 7–9) and F^-, Cl^-, and Br^- ions have been reported to show positive effects. In this paper, we report how the catalytic activity of Nd_2O_3 could be promoted by BaO and BaX_2(X = F, Cl, Br). The interaction of surface oxygen species with CH_4 has also been investigated by means of Raman and CH_4-pulse experiments.

EXPERIMENTAL

The BaO/Nd_2O_3, $BaCl_2$/Nd_2O_3, and $BaBr_2$/Nd_2O_3 catalysts were prepared by impregnating (with constant heating and stirring to dryness) commercial Nd_2O_3 (Sigma Chemicals, purity >99.99%), respectively, with a solution of $Ba(NO_3)_2$ (MERCK, purity >99%), $BaCl_2$, and $BaBr_2$. The BaF_2/Nd_2O_3 catalyst was prepared by grinding the right amount of BaF_2 (Beijing Chemicals, purity >98.6%) with Nd_2O_3. These catalysts were calcined in air at 800°C for 5 h before being ground, tableted, crushed, and sieved into 40 ~ 80 mesh.

The reactions were carried out with 0.5 g of the catalyst in a fixed-bed quartz flow microreactor (ID = 4 mm) at atmospheric pressure. A thermocouple was used to measure the reaction temperatures which were ranging from 600 to 800°C at 50° intervals. A mixture of methane (Hong Kong Oxygen Company, purity 99.5%), air, and nitrogen was passed through the microreactor. The flow-rate of each gas was controlled by a mass flow controller and was 8.3 mL min^{-1} for methane, 16 mL min^{-1} for air, and 25.7 mL min^{-1} for nitrogen; giving a contact time of 0.6 g s mL^{-1}. The exit flow rate was 50 mL min^{-1} as indicated by a flowmeter. The product distribution was determined by a Shimadzu 8A

[1] To whom correspondence should be addressed. E-mail: pctau@hkbu.edu.hk.

0021-9517/98 $25.00

TCD gas chromatograph with Porapak Q and 5A molecular sieve columns. The measurement for catalytic activity was taken after an on-stream time of 1 h at a particular reaction temperature. The reaction products were H_2O, CO, CO_2, C_2H_6, and C_2H_4. A blank reactor showed no activity whatsoever below 800°C. The calculations of methane conversion and selectivity for C_2 were based on total carbon balance (3). A carbon balance of $100 \pm 1\%$ was obtained for every run over the catalysts.

The experiment of oxygen or methane pulsing was conducted in a flow system connected to a Hewlett–Packard G1800A GCD mass quadrupole spectrometer. Helium gas at a flow rate of 10 mL min^{-1} was used as the carrier gas. Each sample (0.2 g) was pretreated in different conditions and then purged with He for 15 min before the O_2- or CH_4-pulse experiment. The pulse volume of gases was 65.7 μL (at 25°C, 1 atm).

The specific surface area of catalyst was measured by means of the BET method. The continuous flow chromatographic technique was adopted with helium as the carrier gas and nitrogen as the adsorbate. The method was based on the amount of nitrogen adsorbed at low temperature (−196°C) and desorbed at higher temperatures.

The phase composition of catalyst before or after the OCM reaction was determined by a X-ray diffractometer (D-MAX, Rigaku) with Cu K_α radiation ($\lambda = 1.542$ Å). The pattern obtained was referred to the powder diffraction file—PDF-2 Database for the identification of crystal structure. X-ray photoelectron spectroscopy (XPS, Leybold Heraeus-Shengyang SKL-12) was performed to characterize the catalyst surface, using Mg K_α as the X-ray source. The binding energies were calibrated to the C *ls* value (284.6 eV) of contaminant carbon. Surface compositions were calculated using the equation

$$X_i = (A_i/S_i) \times 100 \Big/ \sum (A_i/S_i),$$

where A_i is the peak area of XPS signal of element i and S_i is the corresponding atomic sensitivity factor.

Raman experiments were performed using a Nicolet 560 FT Raman spectrometer. The samples were treated in O_2, N_2, H_2, and O_2 successively at different temperatures and were monitored at 25°C without being exposed to air.

For the analysis of chlorine or bromine content, the catalyst was first digested in 0.1 *M* NaOH solution. The resulted solution was neutralized with 2 *M* HNO_3 solution and titrated against standardized $AgNO_3$ solution using 0.005 *M* potassium chromate as indicator (10). In fluorine analysis, the catalyst was dissolved in 6 *M* HNO_3 and distilled water was added to make up a solution of 250 mL. The fluoride ions were detected by an Orion combined fluoride ion selective electrode 900200. The standard solutions used for calibration were prepared from sodium fluoride.

Temperature programmed reduction (TPR) experiments were conducted using a 7% H_2-93% N_2 (v/v) mixture. The flow rate was 50 mL min^{-1} and a thermal conductivity detector was used. Sample weight was 200 mg and the heating rate was 10°C min^{-1}. The catalysts had been treated in O_2 at 800°C for 1 h and cool to RT in O_2 before the TPR experiments were performed.

RESULTS

Catalytic Performances of BaO- and BaX_2-Promoted Nd_2O_3 Catalysts

The catalytic performances (readings were taken 1 h after temperature stabilization) of the 30 mol% BaO- and 30 mol% BaX_2-promoted Nd_2O_3 catalysts were listed in Table 1. At 750°C, pure Nd_2O_3 had a CH_4 conversion of 28.1% and a C_2 selectivity of 33.3%; the corresponding C_2 yield was 9.4%. When 30 mol% BaO was added to Nd_2O_3, CH_4 conversion, C_2 selectivity, and C_2 yield were enhanced to 35.9, 45.4, and 16.3%, respectively. Further increase in C_2 selectivity could be achieved when BaX_2 was used instead of BaO to promote Nd_2O_3. Compared to undoped Nd_2O_3, C_2 selectivity was increased from 33.3 to 50.7% and CH_4 conversion from 28.1 to 42.4% over the 30 mol% $BaCl_2/Nd_2O_3$ catalyst at 750°C, with the C_2 yield more than doubled. Similar promotions were also observed over the 30 mol% BaF_2/Nd_2O_3 and 30 mol% $BaBr_2/Nd_2O_3$ catalysts. The best achievable C_2 selectivity was 54.2% over 30 mol% BaF_2/Nd_2O_3 at 700°C. The reaction rate could also be improved to various extents over the BaO- or BaX_2-promoted Nd_2O_3 catalysts.

BET, XRD, and XPS Studies

From Table 2, one can see that the specific surface area of fresh Nd_2O_3 was 7.4 $m^2\,g^{-1}$. When 30 mol% BaO was added to Nd_2O_3, the specific surface area decreased to 5.7 $m^2\,g^{-1}$. When BaX_2 was used instead of BaO, the area diminished to 2–3 $m^2\,g^{-1}$. After 8 h of OCM reaction, the specific surface areas of the catalysts became even smaller.

The XRD results are listed in Tables 3 and 4. For the fresh 30 mol% BaO/Nd_2O_3 catalyst, besides the dominant hexagonal Nd_2O_3 phase, there were the minor orthorhombic α-$Ba(OH)_2$ and $BaCO_3$ phases. It is understandable because BaO interacts with CO_2 and H_2O in air to form $BaCO_3$ and $Ba(OH)_2$. For the 30 mol% BaF_2/Nd_2O_3 catalyst, there were strong signals of both hexagonal Nd_2O_3 and cubic BaF_2. However, for 30 mol% $BaCl_2/Nd_2O_3$ and 30 mol% $BaBr_2/Nd_2O_3$, only weak lines of orthorhombic $BaCl_2$ and monoclinic $BaBr_2 \cdot 2H_2O$ were detected, respectively, along with the strong lines of hexagonal Nd_2O_3. After 8 h of OCM reaction at 800°C, no new phase was produced in the 30 mol% BaO/Nd_2O_3 and 30 mol% BaF_2/Nd_2O_3 catalysts. However, in 30 mol% $BaCl_2/Nd_2O_3$ and 30 mol%

TABLE 1

The Catalytic Performances of Nd_2O_3 and 30 mol% BaO- and 30 mol% BaX_2(X = F, Cl and Br)-Promoted Nd_2O_3 Catalysts

Catalyst	Temp. (°C)	Conversion (%)	Selectivity (%)		C_2H_4/C_2H_6 ratio	Yield (%)	Reaction rate (10^{-3} mol m^{-2} h^{-1})
			C_2	CO_x			
Nd_2O_3	600	26.0	27.0	73.0	0.7	7.0	8.06
	650	27.6	32.6	67.4	0.9	9.0	8.56
	700	27.9	35.9	64.2	1.0	10.0	8.65
	750	28.1	33.3	66.7	1.0	9.4	8.71
	800	27.2	32.6	67.4	1.6	8.9	8.43
30 mol% BaO/Nd_2O_3	600	32.6	35.5	64.5	0.9	11.6	10.5
	650	36.0	41.1	58.9	1.0	14.8	11.6
	700	36.0	44.8	55.2	1.0	16.2	11.6
	750	35.9	45.4	54.6	1.2	16.3	11.6
	800	31.7	37.4	62.6	2.5	11.9	10.2
30 mol% BaF_2/Nd_2O_3	600	27.4	36.2	63.8	0.7	9.9	13.0
	650	32.8	50.9	49.1	1.1	16.7	15.6
	700	35.0	54.2	45.9	1.2	18.9	16.6
	750	33.8	52.4	47.4	1.2	17.8	16.1
	800	31.8	48.2	51.8	1.5	15.3	15.1
30 mol% $BaCl_2/Nd_2O_3$	600	25.2	22.3	77.7	0.5	5.6	7.07
	650	31.0	34.0	66.0	0.8	10.5	8.68
	700	39.7	47.9	52.1	1.5	19.0	11.1
	750	42.4	50.7	49.3	2.1	21.5	11.9
	800	41.5	47.0	53.0	3.3	19.5	11.6
30 mol% $BaBr_2/Nd_2O_3$	600	28.3	32.0	68.0	1.1	9.0	7.85
	650	35.4	46.3	53.8	1.3	16.4	9.80
	700	36.0	47.6	52.4	1.2	17.1	9.97
	750	35.9	46.9	53.1	1.4	16.8	9.96
	800	33.6	41.2	58.9	2.7	13.8	9.30

Note. $CO_x = CO + CO_2$.

$BaBr_2/Nd_2O_3$, new phases of orthorhombic $Ba_3Cl_4CO_3$ and $Ba_3Br_4CO_3$ were observed. The relative amount of $Ba_3Br_4CO_3$ in 30 mol% $BaBr_2/Nd_2O_3$ was more than that of $Ba_3Cl_4CO_3$ in 30 mol% $BaCl_2/Nd_2O_3$. Table 4 lists the results of lattice parameters of hexagonal Nd_2O_3 in the 30 mol% BaO/Nd_2O_3 and 30 mol% BaX_2/Nd_2O_3 catalysts measured before and after the OCM reaction. The results showed that the lattice of hexagonal Nd_2O_3 had been somewhat enlarged and there were further enlargements during the 8 h of OCM reaction at 800°C.

TABLE 2

The Surface Areas of 30 mol% BaO- and 30 mol% BaX_2-Promoted Nd_2O_3 Catalysts Measured Before and After the OCM Reaction

Catalyst	Before reaction (m^2 g^{-1})	After reaction (m^2 g^{-1})
Nd_2O_3	7.4	1.5
30 mol% BaO/Nd_2O_3	5.7	1.4
30 mol% BaF_2/Nd_2O_3	1.8	0.9
30 mol% $BaCl_2/Nd_2O_3$	3.1	1.6
30 mol% $BaBr_2/Nd_2O_3$	3.1	1.6

XPS spectra of these catalysts recorded before and after the OCM reaction showed Nd 3d5/2 peak at ca 981.7 eV binding energy. The Ba 3d5/2 and O 1s peaks were at ca 779.7 and 531.6 eV, respectively. For the 30 mol% BaX_2/Nd_2O_3 catalysts, F 1s, Cl 2p3/2, and Br 3d5/2 peaks were, respectively, at ca 684.1, 198.5, and 68.9 eV. We did not observe any changes in binding energies of the fluorine, chlorine, and bromine species that would point to lattice substitution for O^{2-} anions. The C 1s spectra showed peaks of CH_x and carbonate at 284.6 and 288.5 eV. After the OCM reaction, we observed a slight increase in C 1s intensity at 288.5 eV. Table 5 shows the surface composition of halide measured before and after the OCM reaction. For homogeneous distribution of BaX_2 in Nd_2O_3, the Ba/Nd and X/Nd ratios should be 0.21 and 0.43, respectively. Since we have higher values of Ba/Nd and X/Nd, we conclude that there was BaX_2 accumulated on the surface of Nd_2O_3. For the 30 mol% BaF_2/Nd_2O_3 catalyst, the Ba/Nd value decreased with reaction time. It was 1.3 for the fresh catalyst. After 8 h, it became 1.0 and was 0.27 at 40 h. Similarly, the F/Nd value decreased from 4.1 to 0.8 after 8 h and was 0 after 40 h. The results suggest that infiltration of Ba^{2+} and F^- ions into the Nd_2O_3 lattice had occurred. As for the 30 mol%

TABLE 3

The XRD Results of 30 mol% BaO- and 30 mol% BaX_2-Promoted Nd_2O_3 Catalysts

Catalyst	Phases (before OCM)	Phases (after OCM)
30 mol% BaO/Nd_2O_3	Hexagonal Nd_2O_3 (s) Orthorhombic α-$Ba(OH)_2$ (w) Orthorhombic $BaCO_3$ (w)	Hexagonal Nd_2O_3 (s) Orthorhombic α-$Ba(OH)_2$ (w) Orthorhombic $BaCO_3$ (w)
30 mol% BaF_2/Nd_2O_3	Hexagonal Nd_2O_3 (s) Cubic BaF_2 (s)	Hexagonal Nd_2O_3 (s) Cubic BaF_2 (s)
30 mol% $BaCl_2/Nd_2O_3$	Hexagonal Nd_2O_3 (s) Orthorhombic $BaCl_2$ (w)	Hexagonal Nd_2O_3 (s) Orthorhombic $BaCl_2$ (w) Orthorhombic $Ba_3Cl_4CO_3$ (w)
30 mol% $BaBr_2/Nd_2O_3$	Hexagonal Nd_2O_3 (s) Monoclinic $BaBr_2 \cdot 2H_2O$ (w)	Hexagonal Nd_2O_3 (s) Monoclinic $BaBr_2 \cdot 2H_2O$ (w) Orthorhombic $Ba_3Br_4CO_3$ (w)

Note. s, strong; w, weak.

$BaCl_2/Nd_2O_3$ and 30 mol% $BaBr_2/Nd_2O_3$ catalysts, the Ba/Nd values decreased, respectively, from 0.60 to 0.59 and 1.40 to 0.92 after 8 h. The corresponding X/Nd values, on the other hand, increased from 1.0 to 1.4 and 1.4 to 1.7. In other words, during the OCM reaction, Ba^{2+} ions were diffusing into Nd_2O_3 while Cl^- and Br^- ions were migrating from the bulk to the surface. Also shown in Table 5 are the comparisons of surface and bulk compositions of halide ions. For 30 mol% BaF_2/Nd_2O_3, the F^- surface composition (2.4 wt%) measured at 8 h was much smaller than that (12.9 wt%) measured before the reaction, although bulk analysis showed that the total loss of fluorine during the OCM reaction was only 0.3 wt% (reduced from 4.0 to 3.7 wt%). For the 30 mol% $BaCl_2/Nd_2O_3$ and 30 mol% $BaBr_2/Nd_2O_3$ catalysts, it was the other way round. Bulk analysis showed that the losses during OCM reactions were 1.4 and 4.4 wt%, respectively, whereas surface analysis revealed that the compositions of the halides on the surfaces were rather similar before and after the reaction.

Effects of $BaCl_2$ Loading and Reaction Time on Catalytic Performance of $BaCl_2$-Promoted Nd_2O_3 Catalysts

Figure 1 shows the variations of CH_4 conversion, C_2 selectivity, and C_2 yield at 750 and 800°C over the $BaCl_2/Nd_2O_3$ catalysts with $BaCl_2$ composition ranging from 0 to 95 mol%. From 0 to 30 mol% $BaCl_2$ loadings, CH_4 conversion and C_2 selectivity increased (from ca 30%) to ca 40 and 50%, respectively, and stayed at these values when $BaCl_2$ loading was above 30 mol%. Optimal C_2H_4/C_2H_6 ratios of ca 5.0 and 12.0 were observed over the catalyst with 70 mol% $BaCl_2$ loading at 750 and 800°C, respectively.

In order to examine the stability of the 30 mol% $BaCl_2/Nd_2O_3$ catalyst, we have done the lifetime experiment of 40 h at 750°C with $CH_4 : O_2 : N_2 = 2.47 : 1 : 11.4$ and contact time $= 0.6$ g s mL^{-1}. The catalyst was rather stable and CH_4 conversion, C_2 selectivity, and C_2 yield stayed at around 40.5, 51.0, and 20.6%, respectively, within the test period. The C_2H_4/C_2H_6 ratio decreased from 2.7 to 2.1 in the first 2 h and remained at around 2.0 thereafter.

Raman Studies

Figure 2 shows the Raman spectra of Nd_2O_3, 30 mol% BaO/Nd_2O_3 and 30 mol% BaX_2/Nd_2O_3 after being treated in O_2 at 800°C for 30 min. There was no peak over Nd_2O_3, implying that no dioxygen species could be generated on Nd_2O_3. With the 30 mol% BaO/Nd_2O_3 catalyst, there were (1) a very strong peak at ca 1042 cm^{-1} and (2) a broad peak

TABLE 4

The Lattice Parameters of Hexagonal Nd_2O_3 in 30 mol% BaO- and 30 mol% BaX_2-Promoted Nd_2O_3 Catalysts

Catalyst	Lattice parameter (Å)	
	Before	After
Nd_2O_3	$a_0 = b_0 = 3.8297$ $c_0 = 5.9987$	$a_0 = b_0 = 3.8297$ $c_0 = 5.9987$
30 mol% BaO/Nd_2O_3	$a_0 = b_0 = 3.8304$ $c_0 = 6.0004$	$a_0 = b_0 = 3.8309$ $c_0 = 6.0007$
30 mol% BaF_2/Nd_2O_3	$a_0 = b_0 = 3.8328$ $c_0 = 6.0013$	$a_0 = b_0 = 3.8332$ $c_0 = 6.0020$
30 mol% $BaCl_2/Nd_2O_3$	$a_0 = b_0 = 3.8310$ $c_0 = 6.0016$	$a_0 = b_0 = 3.8322$ $c_0 = 6.0037$
30 mol% $BaBr_2/Nd_2O_3$	$a_0 = b_0 = 3.8335$ $c_0 = 6.0000$	$a_0 = b_0 = 3.8350$ $c_0 = 6.0019$

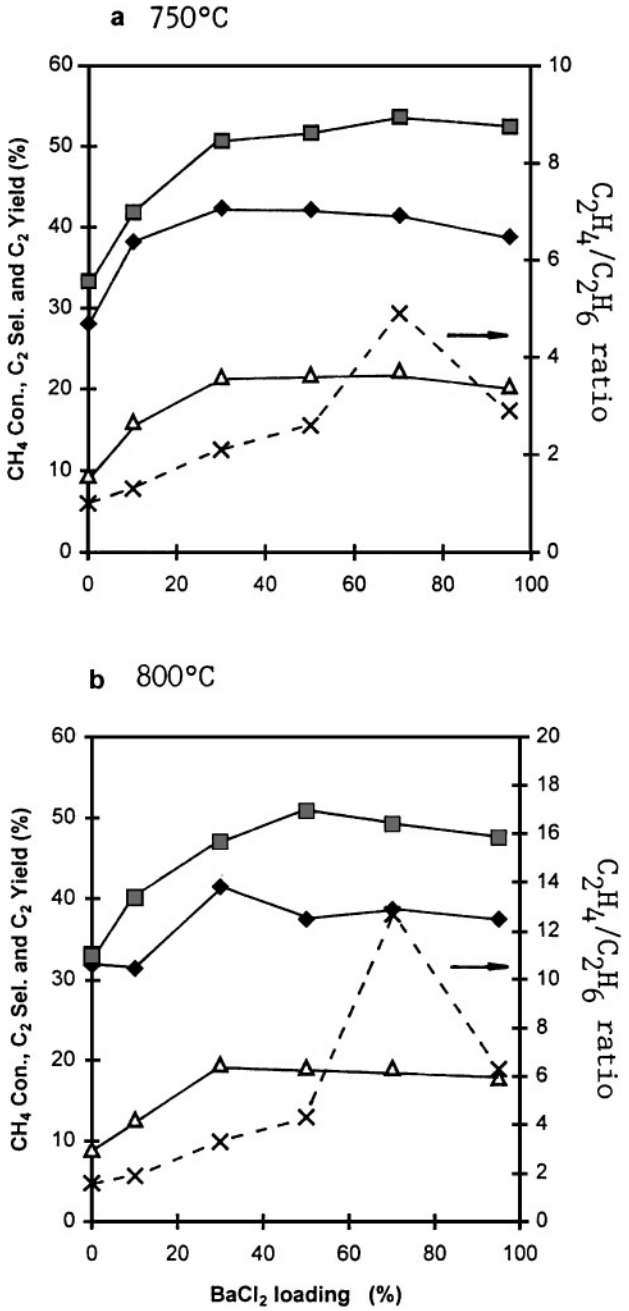

FIG. 1. The catalytic performance of the $BaCl_2/Nd_2O_3$ catalysts at (a) 750 and (b) 800°C related to $BaCl_2$ loading. (◆) CH_4 conversion; (■) C_2 selectivity; (Δ) C_2 yield; (×) C_2H_4/C_2H_6.

centred at 1373 cm^{-1} which can be assigned to O_2^- and $O_2^{\delta-}$ $(0 < \delta < 1)$ species, respectively (5, 6). A weak and narrow peak at 695 cm^{-1} can be assigned to CO_3^{2-}. The detection of carbonate in the 30 mol% BaO/Nd_2O_3 catalyst is in accord with the XRD results (Table 3). Compared to the 30 mol% BaO/Nd_2O_3 catalyst, there were dioxygen species of lesser amounts on the 30 mol% BaX_2/Nd_2O_3 catalysts. Although various dioxygen species existed on the surface of these catalysts, one can observe that the distribution of

TABLE 5

Surface and Bulk Halide Compositions (wt%) of 30 mol% BaX_2/Nd_2O_3 Catalysts

Catalyst	Halogen	Surface		Bulk	
		Before	After[a]	Before	After[a]
30 mol% BaF_2/Nd_2O_3	F	12.9	2.4	4.0	3.7
30 mol% $BaCl_2/Nd_2O_3$	Cl	6.2	6.0	7.0	5.6
30 mol% $BaBr_2/Nd_2O_3$	Br	17.3	17.9	14.2	9.8

[a] After 8 h of OCM reaction at 750°C.

oxygen species differed. For 30 mol% BaF_2/Nd_2O_3, the profile at ca 1000 cm^{-1} was with components at ca 978 and 1050 cm^{-1} and the intensity at 1373 cm^{-1} was very weak, implying that O_2^{2-}, O_2^{n-}, and O_2^- were major dioxygen species on the surface. For the 30 mol% $BaCl_2/Nd_2O_3$ catalyst, there were two peaks at 978 and 1050 cm^{-1}, a shoulder peak at 890 cm^{-1}, and a weak peak at 1373 cm^{-1}, indicating that there were larger amounts of O_2^{n-} and O_2^- and lesser amounts of O_2^{2-} and $O_2^{\delta-}$ species. Furthermore, relatively

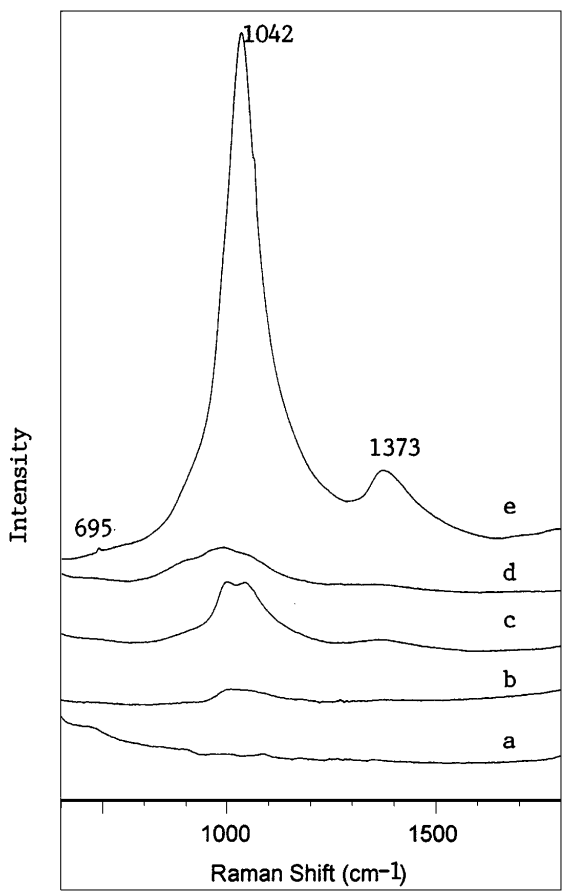

FIG. 2. Raman spectra of the samples after being treated in O_2 at 800°C for 30 min and cooled to 25°C in O_2. (a) Nd_2O_3; (b) 30 mol% $BaBr_2/Nd_2O_3$; (c) 30 mol% $BaCl_2/Nd_2O_3$; (d) 30 mol% BaF_2/Nd_2O_3; (e) 30 mol% BaO/Nd_2O_3.

speaking, only small amounts of O_2^{n-} and O_2^- were observed over the 30 mol% $BaBr_2/Nd_2O_3$ catalyst.

In order to study the stability of these dioxygen species, we treated the catalysts in various conditions and monitored their behaviors. When the 30 mol% BaO/Nd_2O_3 sample (Fig. 3) was heated in N_2 at 800°C for 15 min, the intensities centred at 1042 and 1360 cm^{-1} reduced. Such reduction could be due to O_2 desorption. With the diminution of dioxygen intensities, two peaks at 690 and 1060 cm^{-1} due to CO_3^{2-} emerged. When the sample was treated in H_2 at 600°C for 15 min, the peaks of dioxygen species diminished further and the carbonate peaks became more obvious. Further reduction at 700°C for another 15 min could cause the CO_3^{2-} peaks to disappear, probably due to carbonate decomposition. The dioxygen species could recover completely when the reduced sample was heated in O_2 at 700°C for 15 min, and a new peak appeared at 845 cm^{-1}. Such frequency matches well with that of lattice O–O stretching vibration of pure BaO_2. We hence assign the peak at 845 cm^{-1} to lattice O–O stretching vibration of BaO_2.

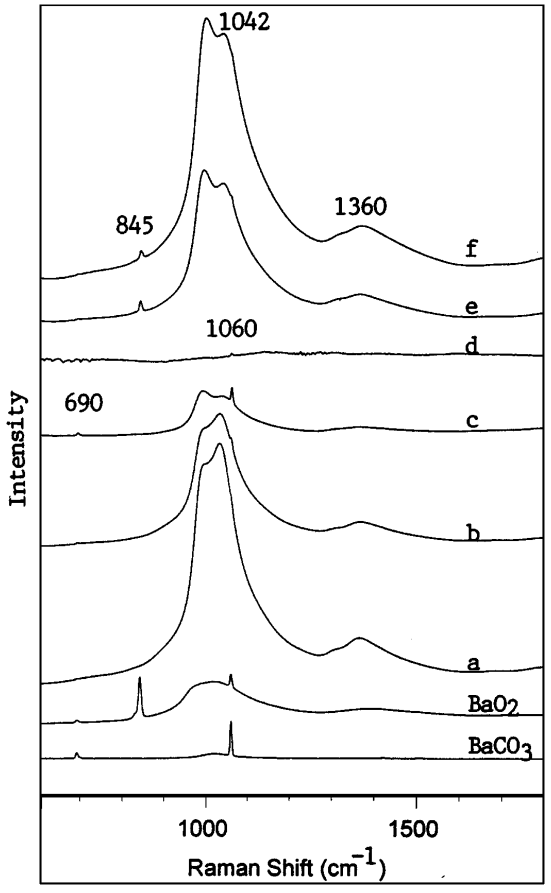

FIG. 3. Raman spectra of 30 mol% BaO/Nd_2O_3. (a) in O_2 at 800°C for 30 min; (b) in N_2 at 800°C for 15 min; (c) in H_2 at 600°C for 15 min; (d) in H_2 at 700°C for 15 min; (e) in O_2 at 600°C for 15 min; (f) in O_2 at 700°C for 15 min. Also shown are the Raman spectra of pure $BaCO_3$ and BaO_2.

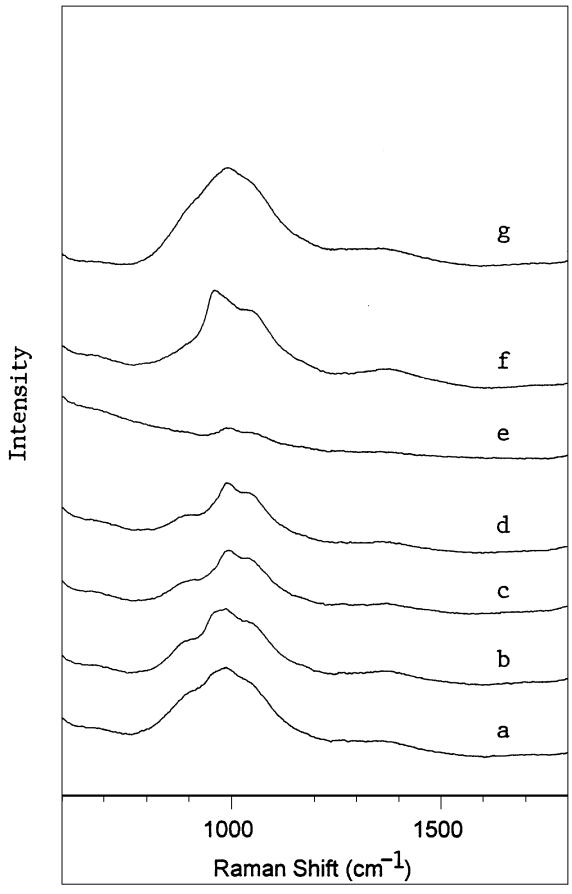

FIG. 4. Raman spectra of 30 mol% BaF_2/Nd_2O_3. (a) in O_2 at 800°C for 30 min; (b) in N_2 at 600°C for 15 min; (c) in N_2 at 800°C for 15 min; (d) in H_2 at 400°C for 15 min; (e) in H_2 at 600°C for 15 min; (f) in O_2 at 600°C for 15 min; (g) in O_2 at 800°C for 15 min.

When oxidised 30 mol% BaF_2/Nd_2O_3 (Fig. 4) was heated in N_2 at 600°C for 15 min, the peaks of the O_2^{2-}, O_2^{n-}, O_2^-, and $O_2^{\delta-}$ species became small. At 800°C in N_2 for 15 min, the peaks became even smaller. The results show that part of the dioxygen species could desorb at high temperatures. When the sample was reduced in H_2 at 400°C for 15 min, the intensities of the dioxygen species did not decrease. At 600°C in H_2 for 15 min, the dioxygen species were largely reduced. When the reduced sample was heated in O_2 at 600°C for 15 min, the peaks of the O_2^{n-}, O_2^-, and $O_2^{\delta-}$ species recovered, with O_2^{2-} being the exception. O_2 treatment at 800°C would result in the complete recovery of the dioxygen peaks.

Similarly, the peak intensities of dioxygen species decreased when the oxidised 30 mol% $BaCl_2/Nd_2O_3$ and 30 mol% $BaBr_2/Nd_2O_3$ samples were heated in N_2 at 800°C for 15 min. The dioxygen species on 30 mol% $BaCl_2/Nd_2O_3$ and 30 mol% $BaBr_2/Nd_2O_3$ disappeared when the samples were heated in H_2 at 600 and 500°C, respectively. The dioxygen species could also recover when the catalysts were heated in O_2 at 800°C.

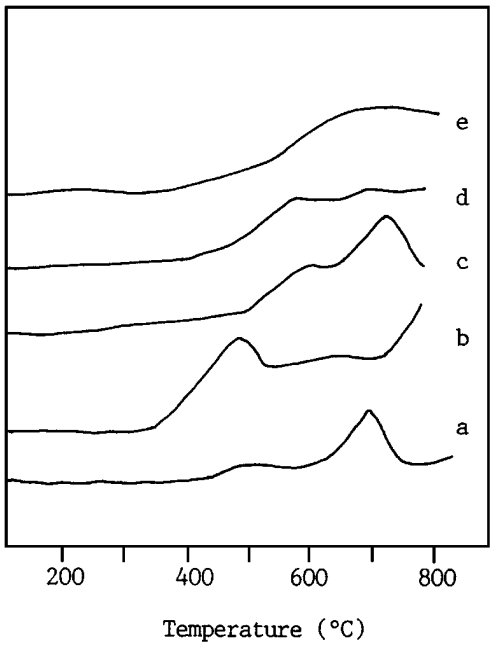

FIG. 5. TPR spectra of (a) Nd_2O_3; (b) 30 mol% BaO/Nd_2O_3; (c) 30 mol% BaF_2/Nd_2O_3; (d) 30 mol% $BaCl_2/Nd_2O_3$; (e) 30 mol% $BaBr_2/Nd_2O_3$.

TPR Studies

Figure 5 shows the TPR spectra of the Nd_2O_3, 30 mol% BaO/Nd_2O_3, and 30 mol% BaX_2/Nd_2O_3 catalysts. There were reducible oxygen species in all the samples. For Nd_2O_3, there were a weak band ranging from 440 to 600°C and a strong one from 600 to 750°C. Since the Raman results indicated that there was no dioxygen species in Nd_2O_3, the two peaks should represent reducible oxygen species other than dioxygen. For 30 mol% BaO/Nd_2O_3, the amount of reducible oxygen species was much larger and reduction started at ca 350°C with bands being observed at ca 480, 640, and above 700°C. For the 30 mol% BaX_2/Nd_2O_3 catalysts, reduction occurred at ca 400°C and carried on well above 700°C. There were two bands at ca 600 and 720°C in the TPR profile of 30 mol% BaF_2/Nd_2O_3. For the 30 mol% $BaCl_2/Nd_2O_3$ and 30 mol% $BaBr_2/Nd_2O_3$ catalysts, reduction started at 420°C and extended to temperatures above 750°C. According to the TPR profiles, one can realize that the amounts of reducible oxygen in the catalysts decrease in the order of 30 mol% BaO/Nd_2O_3 > 30 mol% BaF_2/Nd_2O_3 > 30 mol% $BaCl_2/Nd_2O_3$ > 30 mol% $BaBr_2/Nd_2O_3$ > Nd_2O_3.

Interaction of CH_4 with Oxygen Species

Figure 6 shows the Raman spectra when the 30 mol% BaF_2/Nd_2O_3 catalyst was heated in CH_4 at different temperatures. One can observe that the band centred at ca 1000 cm^{-1} became smaller when the catalyst was heated in pure CH_4 at 600°C for 15 min. When treated in CH_4 at 700°C for another 15 min, the band disappeared completely. The Raman profile could be renewed when the catalyst was treated in O_2 at 700°C for 15 min. When the sample was heated in reaction gas ($CH_4 : O_2 : N_2 = 2.47 : 1 : 11.4$) at 750°C and cooled down to room temperature in reaction gas or N_2, peaks were observed within the 850 to 1400 cm^{-1} region. The results indicate that the dioxygen species were interacting with CH_4 at 600°C over the 30 mol% BaF_2/Nd_2O_3 catalyst. The extent of interaction increased with temperature rise. The dioxygen species consumed in the OCM reaction could be replenished in the presence of gaseous O_2.

In order to identify the effects of dioxygen species on the OCM reaction, we removed the dioxygen species from the catalysts by H_2-reduction and pulsed CH_4 over them. The results were listed in Table 6. When 65.7 μL of CH_4 was pulsed at 750°C over the Nd_2O_3 catalyst which had been treated in O_2 at 800°C, the CH_4 conversion, C_2 selectivity, and C_2H_4/C_2H_6 ratio were 4.5%, 30.0%, and 0.38,

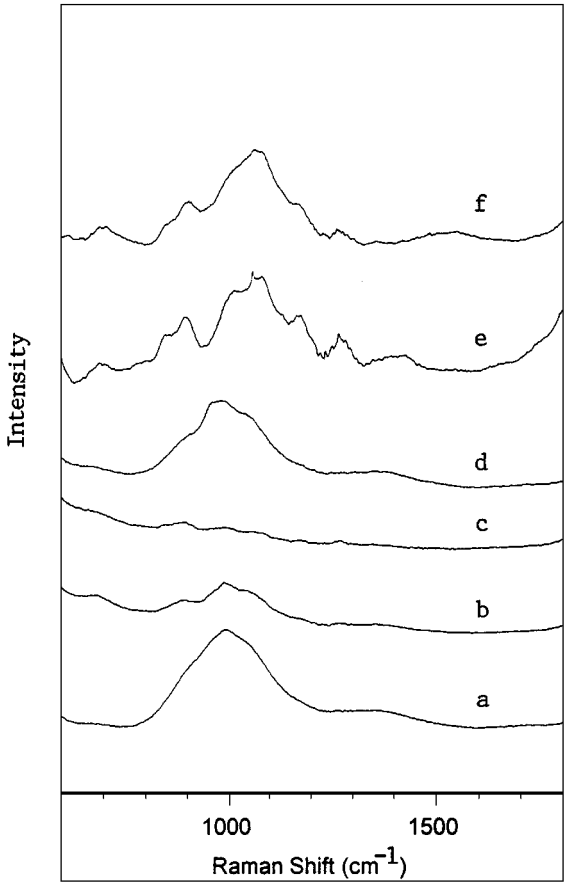

FIG. 6. Raman spectra of 30 mol% BaF_2/Nd_2O_3. (a) in O_2 at 800°C for 30 min; (b) in CH_4 at 600°C for 15 min; (c) in CH_4 at 700°C for 15 min; (d) in O_2 at 800°C for 15 min; (e) in reaction gas ($CH_4 : O_2 : N_2 = 2.47 : 1 : 11.4$) at 750°C for 15 min, then cooled down to room temperature in reaction gas; (f) in reaction gas ($CH_4 : O_2 : N_2 = 2.47 : 1 : 11.4$) at 750°C for 15 min then cooled down to room temperature in N_2.

TABLE 6

The Results of CH_4 Pulse Experiments over BaO- and BaX_2-Promoted Nd_2O_3 Catalysts Treated in O_2 or H_2

Catalyst	Treatment condition	CH_4 con. (%)	C_2 selectivitiy (%)	C_2H_4/C_2H_6 ratio	Yield (%)	CO_x selectivity (%)
Nd_2O_3	in O_2 at 800°C	4.5	30.0	0.38	1.4	70.0
	in H_2 at 600°C	4.7	30.1	0.38	1.4	69.9
30 mol% BaO/Nd_2O_3	in O_2 at 800°C	5.8	57.4	2.00	3.3	42.6
	in H_2 at 700°C	3.6	41.8	0.80	1.5	58.2
30 mol% BaF_2/Nd_2O_3	in O_2 at 800°C	6.0	51.2	0.87	3.1	48.8
	in H_2 at 600°C	4.6	32.7	0.52	1.5	67.3
30 mol% $BaCl_2/Nd_2O_3$	in O_2 at 800°C	5.3	71.5	0.77	3.8	28.5
	in H_2 at 600°C	4.5	60.0	0.60	2.7	40.0
30 mol% $BaBr_2/Nd_2O_3$	in O_2 at 800°C	3.9	60.4	1.20	2.1	39.6
	in H_2 at 500°C	3.7	50.0	1.00	1.9	50.0

Note. $CO_x = CO + CO_2$.

respectively. Over the Nd_2O_3 catalyst treated in H_2 at 600°C, there was no obvious change in performance. For the 30 mol% BaO/Nd_2O_3 catalyst, however, the values of CH_4 conversion, C_2 selectivity, and C_2H_4/C_2H_6 ratio were 5.8%, 57.4%, and 2.0, respectively, at 750°C over the O_2-treated sample but decreased to 3.6%, 41.8%, and 0.8, respectively, over the reduced sample. Similar trends were observed over the 30 mol% BaF_2/Nd_2O_3, 30 mol% $BaCl_2/Nd_2O_3$, and 30 mol% $BaBr_2/Nd_2O_3$ catalysts.

O_2-Pulsing Studies

In order to have a quantitative estimation of the reducible oxygen in the catalysts, we first reduced the catalyst at a desired temperature and then pulsed O_2 over it until there was no observable decrease in O_2-pulse size after passing the catalyst. The viewpoint was based on the assumption that the amount of O_2 absorbed should reflect the amount of oxygen removed. Table 7 shows the amount of O_2 absorbed at 800°C after an O_2-treated (800°C, 20 min, followed by cooling in O_2 to 25°C and helium purging at 25°C) sample was reduced (1 h, followed by He purging for 20 min) at a desire temperature. Also shown in Table 7 are the estimated amount of surface oxygen calculated based on the BET surface area (Table 2) and oxygen surface composition (Table 5) of the catalyst. From Table 7, one can see that, although Nd_2O_3 showed high surface concentration of oxygen atoms (48.6 μmol g^{-1}), only 21.6 μmol g^{-1} could be removed in H_2-reduction at 800°C. The amount of oxygen atoms removed during H_2-reduction at 600°C was 6.8 μmol g^{-1}. In other words, after H_2-reduction at 600°C, the amount of reducible mono-oxygen left was 14.8 μmol g^{-1}. Although there were no dioxygen species on the oxidised Nd_2O_3 sample as indicated by the Raman result (Fig. 2), 6.8 μmol g^{-1} of mono-oxygen could

TABLE 7

A Comparison of the Amount of Surface Oxygen, Total Reducible Oxygen, and Mono-Oxygen Left After H_2-reduction

Catalyst	Surface O (μmol g^{-1})	H_2-reduction temperature (°C)	O absorbed (μmol g^{-1})	Mono-oxygen left after H_2-reduction (μmol g^{-1})
Nd_2O_3	48.6	800	21.6	14.8
		600	6.8	
BaO/Nd_2O_3	34.4	800	55.2	27.4
		700	27.8	
BaF_2/Nd_2O_3	8.4	800	38.2	21.0
		600	17.2	
$BaCl_2/Nd_2O_3$	18.4	800	30.2	14.2
		600	16.0	
$BaBr_2/Nd_2O_3$	14.4	800	19.2	17.2
		500	2.2	

Note. The loadings of BaO, BaF_2, $BaCl_2$, and $BaBr_2$ were 30 mol%. All concentrations are expressed in μmol of oxygen atoms per gram of catalyst.

be removed during H_2-reduction at 600°C. The estimated surface concentration of BaO/Nd_2O_3 was 34.4 μmol g^{-1}. When BaX_2 was used, instead of BaO, the surface concentration of oxygen atom decreased by more than 50%. The amount of oxygen atoms removed (in μmol g^{-1}) during H_2-reduction at 800°C decreased in the order of BaO/Nd_2O_3 (55.2) > BaF_2/Nd_2O_3 (38.2) > $BaCl_2/Nd_2O_3$ (30.2) > Nd_2O_3 (21.6) > $BaBr_2/Nd_2O_3$ (19.2). Compared to the surface concentrations of oxygen atoms on the corresponding catalysts, the oxygen removed during H_2-reductions at 800°C from the Nd_2O_3, 30 mol% BaO/Nd_2O_3, and 30 mol% BaX_2/Nd_2O_3 catalysts should be from the surface as well as from the bulk. At lower reduction temperatures (500, 600, or 700°C), the amounts of oxygen removed were less than the corresponding surface oxygen detected on the Nd_2O_3, 30 mol% BaO/Nd_2O_3, 30 mol% $BaCl_2/Nd_2O_3$, and 30 mol% $BaBr_2/Nd_2O_3$ catalysts. Compared to the surface concentration of oxygen on 30 mol% BaF_2/Nd_2O_3 (8.4 μmol g^{-1}), the amount of oxygen atoms removed in H_2-reduction at 600°C (17.2 μmol g^{-1}) was much larger. This is a clear indication that oxygen atoms could also be removed from the bulk. After H_2-reduction at temperatures with no dioxygen species being detected in Raman recordings (Figs. 3, 4), the amounts of reducible mono-oxygen left in the catalysts ranged from 14.2 to 27.4 μmol g^{-1}.

DISCUSSION

Catalytic performance could be improved when 30 mol% BaO was added to Nd_2O_3. When 30 mol% BaX_2(X = F, Cl, Br) was used instead, the catalytic performance was even better (Table 1). The results show that not only the Ba^{2+} ions but also the halide ions were involved in the promotion of Nd_2O_3. Based on the XRD results (Table 4), one can see that the lattice of hexagonal Nd_2O_3 enlarged when 30 mol% BaO or 30 mol% BaX_2 was added to Nd_2O_3. Such lattice enlargement was due to ionic exchange occurred between the Ba^{2+} (1.43 Å) and Nd^{3+} (0.995 Å) ions. Kaminsky *et al.* have studied the Ba-doped yttria oxidative coupling catalyst and proposed that the active sites were charge-deficient oxygen created as Ba^{2+} substituted into Y^{3+} lattice sites (2). Osada *et al.* have also reported that ionic exchange between Ca^{2+} and Y^{3+} would generate active sites for the OCM reaction in the binary oxides of Y_2O_3–CaO (1). Compared to the 30 mol% BaO/Nd_2O_3 case, the lattice parameters of hexagonal Nd_2O_3 in 30 mol% BaX_2/Nd_2O_3 were even larger, possibly due to exchange between X^- (F^- = 1.38 Å, Cl^- = 1.81 Å, and Br^- = 1.95 Å) and certain O^{2-} (1.40 Å) ions. The decrease in coulombic forces after the substitutions would add to the enlargement. The extent of the ionic exchange between X^- and O^{2-} decreased with the increase in halide size. Generally speaking, compared to F^- ions, the Cl^- and Br^- ions are less likely to replace O^{2-} ions. As discussed previously, such ionic exchanges or substitutions would result in the generation of lattice defects in the hexagonal Nd_2O_3 phase.

Among the 30 mol% BaX_2/Nd_2O_3 catalysts, the $BaCl_2$-promoted one showed the best performance; CH_4 conversion of 42.4%, C_2 selectivity of 50.7%, C_2 yield of 21.5%, and C_2H_4/C_2H_6 ratio of 2.1 were obtained at 750°C (Fig. 1). After OCM reaction at 750°C for 40 h, the CH_4 conversion, C_2 selectivity, C_2 yield, and C_2H_4/C_2H_6 ratio stayed at around 40.5, 51.0, 20.6%, and 2.1, respectively; only slight reductions in CH_4 conversion and C_2H_4/C_2H_6 ratio were observed. According to the XPS results (Table 5), surface composition of F^- ions on 30 mol% BaF_2/Nd_2O_3 decreased from 12.9 to 2.4 wt% in 8 h of reaction time. The composition of Cl^- ions on 30 mol% $BaCl_2/Nd_2O_3$ decreased only a little, from 6.2 to 6.0 wt%. Similar to the $BaCl_2$-promoted catalyst, the composition of Br^- ions on 30 mol% $BaBr_2/Nd_2O_3$ only showed very small diminution. However, the results of chemical analysis revealed that there were losses in halide content during the OCM reaction (Table 5). The F, Cl, and Br compositions of the catalysts decreased from 4.0 to 3.7 wt%, 7.0 to 5.6 wt%, and 14.2 to 9.8 wt%, respectively. It is obvious that the F^- ions are more resistant to leaching than the Cl^- or Br^- ions. Halogen loss was due to CO_2 and H_2O interactions with halide ions to produce HX which escaped at high temperatures. Because of the substantial losses in Cl^- and Br^-, new phases of $Ba_3Cl_4CO_3$ and $Ba_3Br_4CO_3$ were formed in the 30 mol% $BaCl_2/Nd_2O_3$ and 30 mol% $BaBr_2/Nd_2O_3$ catalysts, respectively, during OCM reaction (Table 3). Since the loss of fluoride ions was small, $Ba_3F_4CO_3$ was not formed. Usually, dopant ions with smaller ionic radii tend to diffuse into the bulk of the host crystal while dopant ions with larger ionic radii segregate to the surface or the near surface region (11). Of the three halide ions, F^- is the smallest and Br^- is the largest. The F^- ions diffused into the bulk of the catalyst during OCM reaction, resulted in the decrease in surface F^- composition. Both Cl^- and Br^-ions segregated to the surfaces, replenishing the surface with Cl^- and Br^- during OCM reaction. That is why the Br^- and Cl^- surface compositions did not decrease significantly while there were losses in halogens from the catalysts during the OCM reaction.

Based on the Raman results (Fig. 2), no dioxygen species existed on the surface of Nd_2O_3. When 30 mol% BaO was added, dioxygen species were detected in large quantities on 30 mol% BaO/Nd_2O_3. Various dioxygen species existed on the 30 mol% BaX_2/Nd_2O_3 catalysts as well. Nd_2O_3 lattice enlargement, a result of ionic exchange between the Nd^{3+} and Ba^{2+}, as well as X^- and O^{2-} ions in these catalysts, has been detected by XRD, implying that there were lattice defects such as anion vacancies, trapped electrons, and charge-deficient oxygen in the promoted Nd_2O_3 catalysts. Lattice defects of Y_2O_3 have been detected by Osada *et al.* in the Y_2O_3–CaO catalysts (1). They suggested that gaseous oxygen could adsorb on these defect sites to form

electron-deficient oxygen species to be detected by EPR. Kaminsky *et al.* (2) found that lattice defects were created as Ba^{2+} substituted into Y^{3+} lattice sites in Ba/Y_2O_3 catalysts. These lattice defects could adsorb gaseous oxygen to form charge-deficient oxygen sites. In our previous studies, we found that similar substitutions inside the 20 mol% SrF_2/SmOF catalyst would induce the formation of lattice defects (12). In the 5 mol% Y_2O_3/BaF_2 catalyst, trapped electrons and O_2^- ions could be detected by EPR (4). That trapped electrons on the surface of catalysts could combine with molecular oxygen to form partially reduced oxygen species has been suggested by Ito *et al.* (13) and Wang and Lunsford (14). In the 30 mol% BaO/Nd_2O_3 and 30 mol% BaX_2/Nd_2O_3 catalysts, the formation of dioxygen species was interpreted as being due to the adsorption of gaseous oxygen on lattice defect sites. Because there were no such lattice defects in Nd_2O_3, no dioxygen species were formed.

From Figs. 3 and 4, one can see that part of the dioxygen species could desorb when the samples were treated in N_2 at 800°C. The oxygen species left on the surfaces were thermally stable. They could, nevertheless, be reduced by H_2 at temperatures ranging from 500 to 700°C. When the reduced samples were heated in O_2 at temperatures such as 700 or 800°C, the dioxygen species could be renewed. TPR results (Fig. 5) showed that there were reducible oxygen species in these samples after the dioxygen species were completely reduced. For the 30 mol% BaO/Nd_2O_3 sample, there were oxygen species to be reduced well above 700°C. For the 30 mol% BaX_2/Nd_2O_3 catalysts, there were reductions above 600°C. Although there was no dioxygen species on the surface of Nd_2O_3, there was reducible oxygen. We hence suggest that besides the Raman-detectable dioxygen, there were mono-oxygen species such as O^- present to be reduced by H_2.

Although methane can be activated at lower temperatures by certain oxygen species on the surface, it is known that the OCM reaction generally proceeds at temperatures above 600°C. At such temperatures, the adsorbed oxygen species (e.g., $O_2^{\delta-}$, O_2^-, O_2^{n-}, O_2^{2-}, and O^-) are capable of abstracting hydrogen from methane to generate methyl radicals. Lunsford *et al.* suggested that O^- species were the active centres for the OCM reaction in Li^+/MgO catalyst (15). Aika and Lunsford also reported that CH_4 could interact with O^- species on the surface of MgO to produce C_2H_4 and CO_2 at −130–150°C and C_2H_4 could interact with O^- species (16, 17). These results showed that O^- species could be sites for CH_4 activation. Later, Lunsford *et al.* detected the existence of O_2^{2-} species on the surface of 4 mol% Ba/MgO catalyst at 800°C by Raman spectroscopy and on the surface of Li^+/MgO catalyst at 750°C by XPS (18, 19). They suggested that the active centres for OCM were in fact the O_2^{2-} species, rather than the O^- species, as suggested before. Otsuka and co-workers have found that C_2 hydrocarbon products could be generated at 400°C when CH_4 reacted with peroxides such as BaO_2, SrO_2, and Na_2O_2 and reported that CH_4 did not interact with O_2^- at such a low temperature (20). They suggested that O_2^{2-} were active oxygen species for the OCM reaction. Korf *et al.* have reported a synergistic effect between Ca and Ba oxides and O_2^{2-} was suggested to be the active oxygen species (21). Osada *et al.* have studied the Y_2O_3–CaO catalysts for the OCM reaction; the increase in C_{2+} selectivity at 600 and 700°C was attributed to interstitial oxygen ions O_2^- (1).

From Fig. 6, the peaks of dioxygen species on the surface of the 30 mol% BaF_2/Nd_2O_3 catalyst became smaller when the sample was heated in CH_4 at 600°C. The peaks disappeared entirely in CH_4 at 700°C. The results revealed that the dioxygen species began to interact with CH_4 at 600°C and was consumed completely at 700°C. However, the peaks did not vanish when the sample was heated in reaction gas ($CH_4 : O_2 : N_2 = 2.47 : 1 : 11.4$) at 750°C. The results showed that the dioxygen species reduced by CH_4 on the surface could be replenished rather efficiently in the presence of gaseous O_2.

Based on the data in Table 6, the Nd_2O_3 catalyst before or after H_2-reduction at 600°C behaved rather similarly in the CH_4-pulsing experiments. From Table 7 and the TPR profile of Nd_2O_3, we know that only a portion of mono-oxygen species had been reduced at 600°C and such loss did not affect the results of CH_4 interaction. For the 30 mol% BaO/Nd_2O_3 and 30 mol% BaX_2/Nd_2O_3 catalysts, however, CH_4 conversion, C_2 selectivity, and C_2H_4/C_2H_6 ratio obviously decreased after the catalysts had been reduced by H_2. Raman results (Figs. 3, 4) showed that the dioxygen species disappeared after the 30 mol% BaO/Nd_2O_3 and 30 mol% BaX_2/Nd_2O_3 catalysts had been reduced by H_2 at 600 or 700°C. Based on the data in Table 7, we conclude that the dioxygen species were on the surface. The TPR results (Fig. 5) suggested that there were still reducible mono-oxygen species in the catalysts after the dioxygen species had been removed by H_2-reduction. In other words, the catalysts with both dioxygen and mono-oxygen showed better performances than those with only mono-oxygen. According to the results, we can be sure that both dioxygen and mono-oxygen on the surfaces can activate CH_4. The presence of dioxygen species on the surfaces, nevertheless, could significantly enhance the catalytic performance, especially in C_2 selectivity and C_2H_4/C_2H_6 ratio.

CONCLUSION

Based on the catalytic performance of the BaO/Nd_2O_3 and BaX_2/Nd_2O_3 (X = F, Cl, Br) catalysts, we know that BaO could enhance the catalytic performance of Nd_2O_3 while BaX_2 could further improve the C_2 selectivity in the OCM reaction. Part of the halide ions in the 30 mol% BaX_2/Nd_2O_3 catalysts leached during the OCM reaction.

The F^- was the most resistant to leaching. The generation of dioxygen species could be related to lattice distortions. Due to ionic exchanges between the Ba^{2+} and Nd^{3+} as well as the X^- and O^{2-} ions, there were Nd_2O_3 lattice distortions, implying that there were defects in the BaO/Nd_2O_3 and BaX_2/Nd_2O_3 catalysts. On Nd_2O_3, there was only mono-oxygen, whereas there were both dioxygen and mono-oxygen species on 30 mol% BaO/Nd_2O_3 and 30 mol% BaX_2/Nd_2O_3. Both dioxygen and mono-oxygen species could activate methane. At high temperatures, the presence of dioxygen species could obviously improve the catalytic performance of the OCM reaction, noticeably in C_2 selectivity and C_2H_4/C_2H_6 ratio.

ACKNOWLEDGMENTS

The project was supported by the Hong Kong Baptist University (HKBU) and the Hong Kong Research Grants Council, UGC (HKBU 146/95P). Y.W.L. thanks the HKBU for a Ph.D. studentship.

REFERENCES

1. Osada, Y., Koike, S., Fukushima, T., Ogasawara, S., and Shikada, T., *Appl. Catal.* **59**, 59 (1990).
2. Kaminsky, M. P., Zajac, G. W., Campuzano, J. C., Faiz, M., Beaulaige, L., Gofron, K., Jenning, G., Yao, J. M., and Saldin, D. K., *J. Catal.* **136**, 16 (1992).
3. Au, C. T., Liu, Y. W., and Ng, C. F., *J. Catal.* **171**, 231 (1997).
4. Au, C. T., Zhou, X. P., Liu, Y. W., Ji, W. J., and Ng, C. F., *J. Catal.* **174**, 153 (1998).
5. Au, C. T., and Zhou, X. P., *J. Chem. Soc., Faraday Trans.* **93**(3), 485 (1997).
6. Au, C. T., Zhou, X. P., and Wan, H. L., *Catal. Lett.* **40**, 101 (1996).
7. Fujimoto, K., Hashimoto, S., Asami, K., Omata, K., and Tominaga, H., *Appl. Catal.* **50**, 223 (1989).
8. Burch, R., Squire, G. D., and Tsang, S. C., *Appl. Catal.* **46**, 69 (1989).
9. Burch, R., Chalker, R. S., and Loader, P., in "Studies in Surface Science and Catalysis, Vol. 75, New Frontiers in Catalysis" (L. Guczi *et al.*, Eds.), p. 1079. Elsevier, Amsterdam, 1992.
10. Vogel, A. I., "Vogel's Textbook of Quantitative Inorganic Analysis," 5th ed. Longman, Harlow, 1991.
11. Zhang, Z. L., Verykios, X. E., and Baerns, M., *Catal. Rev. Sci. Eng.* **36**(3), 507 (1994).
12. Au, C. T., and Zhou, X. P., *J. Chem. Soc., Faraday Trans.* **92**, 1793 (1996).
13. Ito, I., Kato, M., Toi, T., Shirakawa, T., Ikemoto, I., and Tukuda, T., *J. Chem. Soc., Faraday Trans.*1 **81**, 2835 (1985).
14. Wang, J. X., and Lunsford, J. H., *J. Phys. Chem.* **90**, 5883 (1986).
15. Driscoll, D. J., Wilson, M., Wang, J. X., and Lunsford, J. H., *J. Am. Chem. Soc.* **107**, 58 (1985).
16. Aika, K., and Lunsford, J. H., *J. Phys. Chem.* **82**, 1794 (1978).
17. Aika, K., and Lunsford, J. H., *J. Phys. Chem.* **81**, 1393 (1977).
18. Lunsford, J. H., Yang, X., Haller, K., Laane, L., Mestl, G., and Knozinger, H., *J. Phys. Chem.* **97**, 13810 (1993).
19. Lunsford, J. H., "Natural Gas Conversion II" (H. E. Curry-Hyde and R. F. Howr, Eds.), p. 1. Amsterdam, Elsevier, 1994.
20. Otsuka, K., Said, A. A., Jinno, K., and Komatsu, T., *Chem. Lett.* 77 (1987).
21. Korf, S. J., Roos, J. A., Derksen, J. W. H. C., Vreeman, J. A., Van Ommen, J. G., and Ross, J. R. H., *Appl. Catal.* **59**, 291 (1990).